RESEARCH ARTICLE

Allicin induces post-translational modifications of p53, DNA damage, and oxidative stress in human embryonic kidney cells

Nicole M. Narain[1], Daniel G. Amoako[1, 2, *], Anou M. Somboro[1, 2], Isaiah Arhin[1, 2], Ndumiso N. Mhlongo[1], Hezekiel M. Kumalo[1], Rene B. Khan[1, *]

[1]Medical Biochemistry, School of Laboratory Medicine and Medical Sciences, University of KwaZulu-Natal, Howard Campus, Durban, South Africa. [2]Biomedical Resource Unit, School of Laboratory Medicine and Medical Sciences, College of Health Sciences, University of KwaZulu-Natal, Durban, South Africa.

Received: June 12, 2021; **accepted:** August 2, 2021.

Allicin derived from garlic has been exploited as a therapeutic intervention in the alleviation of fatal diseases. However, its molecular effect on the kidney is yet to be elucidated. This study aimed to determine the toxicity of allicin by assessing the oxidative and apoptotic pathways in human embryonic kidney (HEK293) cells. The HEK293 cells were cultured until confluent in complete culture medium, then treated with the aqueous allicin extract for 24 hours. Cytotoxicity was determined using the 3-(4,5-dimethylthiazol-2-yl)2,5-diphenyl-2H-tetrazolium bromide (MTT) assay. Nitrates and lipid peroxidation assays were performed to assess the generation of free radicals and reactive oxygen/nitrogen species. Luminometry was used to assess caspase activation and adenosine triphosphate concentration. Fragmentation of DNA was measured utilizing the comet assay and confirmed through Hoechst staining. Additionally, protein expressions of nuclear factor erythroid 2-related factor 2 (Nrf2), superoxide dismutase 2 (SOD2), Bcl-2 associated X-protein (Bax), tumor protein p53, and Poly (ADP-ribose) polymerase 1 (PARP-1) were examined by Western blotting assay. Cell viability was decreased with increasing allicin concentration. Although the antioxidant SOD2 and its regulator Nrf2 were upregulated, the higher concentrations of allicin incited its oxidant capacity. This was affirmed by a dose-dependent increase in both reactive nitrogen species and reactive oxygen species that overwhelmed allicin's antioxidant effects and resulted in oxidative stress. Additionally, allicin induced apoptosis *via* caspase activation, adenosine triphosphate stimulation, cleavage of PARP-1, and up-regulation of Bax. Fragmentation of DNA was confirmed by increased comet tail length and the apoptotic cells displayed in the Hoechst assay. Moreover, allicin treatment downregulated the expression of p53 while upregulating PARP-1. Allicin is cytotoxic to HEK293 cells *via* oxidative stress and apoptotic cell death.

Keywords: allicin; apoptosis; cytotoxicity; HEK293 kidney cells; oxidative stress.

[*]**Corresponding author:** Rene B. Khan and Daniel G. Amoako, Medical Biochemistry, School of Laboratory Medicine and Medical Sciences, University of KwaZulu-Natal, Howard Campus, Durban, South Africa. Phone: +27 73 200 1919. Email: myburgr@ukzn.ac.za, amoakodg@gmail.com.

Introduction

A prominent shift from pharmaceutical drugs as therapeutic agents has inclined toward ancient practices of utilizing medicinal plants [1]. These are found to have advantageous traits, beneficial to one's needs. Specifically, the bioactive compounds in these natural remedies modulate a variety of disorders and life-threatening diseases [2]. Examples are organosulfur

compounds present in plants, which have been cultivated for their medicinal use [3]. The pungent smell of organosulfur compounds is attributed to the presence of sulfur groups. Dietary intake of sulfur in humans can be acquired through multiple sources, such as cabbage, onion, broccoli, and garlic among others [4, 5]. Garlic belongs to the Allium genus containing s-alk(en)yl-L-cysteine sulfoxides and is similarly associated with leeks and onions [6, 7]. Although distinguished as a culinary "flavorant", garlic has become accredited as a curative agent in the treatment of diverse pathologies including diabetes [4], hypertension [4], cancer [5], and microbial infections [5]. When fresh, uncooked garlic which is abundant in allicin is crushed, it releases alliinase, an enzyme that facilitates the conversion of alliin to allicin. Allicin explicitly serves as the chief bioactive component in garlic which is beneficial for the treatment of various diseases and is largely dependent on concentration [1, 8]. The decomposition and metabolism of allicin yields therapeutic compounds such as diallyl disulfide, diallyl trisulfide, and diallyl tetrasulfide [8].

Owing to the presence of thiosulfinate groups, allicin has been described as a reactive sulfur species with oxidizing properties and therefore it is able to oxidize thiol-groups such as cysteine and glutathione in cells. The morphology of the protein can then be altered due to the oxidized protein thiols, for example, the development of disulfide bonds [9]. Commonly, the cytosol in healthy cells is in a reduced state (negative redox potential); consequently, a loss or gain of protein function can be incurred as a result of the redox-stimulated morphological variations [10]. While the chemistry of allicin is indicative of its oxidant properties, in reduced quantities it exhibits a role as an antioxidant at physiological echelons [11]. This can be expounded with the knowledge that detoxification enzymes of phase 2 are produced by the minor oxidative surroundings [1]. Minimal amounts of reactive oxygen species (ROS) are required for normal cell maintenance *i.e.* proliferation, gene expression, and host protection [12]. As per customary physiological processes, cells maintain a healthy balance between the oxidant and antioxidant molecules, and so ROS levels remain regulated. Copious ROS production would, therefore, result in the perturbation of this balance, thus resulting in oxidative stress. Oxidative damage to DNA, lipids, and proteins is an inevitable outcome of this imbalance. In accordance with the disruption of this scale, an overproduction of ROS would imply a decline in the production of antioxidant molecules such as glutathione (GSH). Sulfur-containing molecules assist in the replenishment of these antioxidants [12, 13]. In this way, the antioxidant capacity of allicin ensures that there is a deference of oxidative DNA, lipid, and protein modification [13]. These actions result from the ability of allicin to scavenge ROS, elevate the expression of certain first-line defense cellular antioxidants such as superoxide dismutase (SOD2), and supplement GSH levels inside normal cells [13-15]. Additionally, studies have shown that allicin displayed its antioxidant role by upregulating nuclear factor (erythroid-derived 2)-like 2 (Nrf2), the protein responsible for the regulation of essential antioxidant enzymes [16-18]. Although allicin can exhibit beneficial antioxidant responses in lower doses, the redox reaction with cysteine residues might give insight to allicin's toxicity. The ability of allicin to react with cysteine may inhibit the function of enzymes or molecules with available reactive cysteines; for example, reaction with the cysteine residue of GSH may contribute to oxidative stress. Furthermore, the change of cellular redox potential has been associated with apoptotic initiation in different cell types. This has been demonstrated in studies where allicin was shown to cause both cysteine-aspartic proteases (caspase) – dependent and caspase-independent cell death [1, 8, 17].

Caspases are key enzymes involved in the initiation and execution of apoptosis, a programmed series of events characterized by pyknosis (cell shrinkage), blebbing leading to apoptotic bodies and phagocytosis of these bodies [18]. It occurs *via* two main pathways including extrinsic or intrinsic (mitochondrial)

pathways. Initiator caspases 8 and 9 activations results in executioner caspase 3/7 activation. DNA fragmentation is a result of caspase-activated DNase (CAD) which is formed when caspase 3/7 instigates the dissociation of an inhibitor of CAD (iCAD) from CAD, enabling the degradation of chromosomal DNA [17]. Additionally, caspase 3/7 inhibits the novel DNA repair enzyme poly ADP ribose polymerase (PARP), so that no repair can be facilitated [19].

Given that allicin possesses many useful properties and plays a role in modulating lethal diseases, especially in kidney disease, the cytotoxic effect should be evaluated before its application for therapeutic use. Therefore, this study aimed to determine the toxic effect of allicin on HEK293 cells by assessing the oxidative and apoptotic pathways.

Materials and methods

Cell culture

The HEK293 cells were originally obtained from American Type Culture Collection and were acquired from the School of Science and Agriculture (University of Kwa-Zulu Natal, Durban, South Africa). Cryopreserved HEK293 cells were thawed and reconstituted by immersion in 5 mL of complete culture medium (CCM) which was comprised of Dulbecco's Modified Eagles Medium (Lonza, Basel, Switzerland), supplemented with 10% fetal calf serum (Gibco, Waltham, Massachusetts, USA), 1% L-glutamine (Lonza, Basel, Switzerland), and 1% penicillin-streptomycin fungizone (Lonza, Basel, Switzerland) in sterile 50 mL cell culture flasks. The cells were incubated in a 37°C incubator with 5% CO_2 facility. The CCM was changed routinely until confluency was reached. Confluent flasks of cells were washed with Phosphate Buffered Saline (PBS); the cells were dislodged by gentile agitation and counted using the trypan blue method. Cell numbers were then adjusted for the various assays or cryopreserved for later use.

Allicin treatment

Allicin was purchased from a local herbal store. A stock solution of allicin was made by dissolving 750 µg of allicin in 2.5 mL of Complete Culture Medium (CCM) (300 µg/mL), which was, thereafter, centrifuged at 2,500 rpm for 5 min to pellet any residual particles. The supernatant was used to prepare the HEK293 cell treatments. After 24 h treatment, the treated cells and treatment media were retained for use in the respective assays.

The 3-(4, 5-dimethylthiazol-2-yl) 2, 5-diphenyl-2H-tetrazolium bromide (MTT) assay

The colorimetric cell viability assay was used to determine the cytotoxicity and half-maximum inhibitory concentration (IC_{50}) of allicin in HEK293 cells [20–22]. Suspended HEK293 cells were dispensed into a 96-well plate in triplicate (15,000 cells/well, 300 µL/well) and incubated overnight to adhere. Treatments were then prepared with a range of allicin concentrations (0, 2, 4, 8, 12, 16, 41, 81, 122, 162, 203, 243 µg/mL) and incubated under the same conditions for 24 h. The concentration range was calculated based on previous experimental works [19].

The MTT salt solution was prepared (5 mg/mL in 0.1 M PBS) (Sigma, Johannesburg, South Africa), and 800 µL was added to 4 mL of CCM. The treatment medium was discarded and replaced with 120 µL of the MTT solution. After 4 h incubation at 37°C, the MTT solution was discarded and 100 µL of dimethyl sulfoxide (Sigma, Johannesburg, South Africa) was added to each well for solubilization of the formazan crystal. It was then incubated for 1 h at 37°C. The optical density at 570 nm/690 nm was determined using the Bio-Tek Quant MQ×200 spectrophotometer (Winooski, Vermont, USA). Graphpad Prism v5.0 (GraphPad Software Inc., La Jolla, California, USA) was used to plot cell viability of the samples and the log concentration relative to the control to produce the IC_{50} which was halved to produce a less concentrated test solution, namely IC_{25}. For subsequent assays, confluent HEK293 cells were treated with IC_{25} and IC_{50} concentrations of allicin for 24 h; control

cells received CCM only. The treatment medium was retained for later use.

Adenosine triphosphate (ATP) assay

The concentration of intracellular ATP was measured *via* the CellTiter-Glo® assay [20, 21]. Duplicate wells of treated cells (20,000 cells in 50 µL of PBS) were prepared with PBS as the blank. The addition of 50 µL of the CellTiter-Glo® reagent (Promega, Madison, Wisconsin, USA) into each well was followed by incubation of the plate in the dark for 30 min at room temperature. After the incubation period, ATP activity was detected with the Modulus™ microplate luminometer (Turner Bio-systems, Sunnyvale, California, USA) and was recorded in relative light units (RLU).

Caspase activity

The Caspase-Glo® assay was used to assess the activities of caspases 8, 9, and 3/7, which are the initiator and executioner caspases of apoptosis, respectively [20–22]. To a white opaque 96 well luminometer plate, 50 µL of 0.1 M PBS (blank) and cell suspension (20,000 cells/well in 50 µL 0.1 M PBS) were plated in duplicate. Caspase-Glo®-3/7, -8, and -9 reagents (Promega, Madison, Wisconsin, USA) were reconstituted according to the manufacturer's instructions, and 50 µL of each of these were added into respective wells. The plate was wrapped in foil and after a 30-minute incubation at room temperature in the dark, luminescence was detected *via* the Modulus™ microplate luminometer and expressed as RLU.

Comet assay

The alkaline comet assay was used to detect DNA fragmentation induced by allicin in HEK293 cells [20–22]. Two frosted end microscope slides were prepared for each sample. Concisely, 800 µL of 2% low-melting point agarose (LMPA) was pipetted onto the labeled slides, held in place by a coverslip and polymerized for 10 min at 4℃. Likewise, the second layer consisting of gel red (1 µL), cell suspension (20,000 cells in 30 µL of 0.1 M PBS), and 1% LMPA (400 µL); and the third layer containing 400 µL of 1% LMPA were prepared. The final coverslips were removed, and the slides were immersed in lysis buffer (100 mM EDTA, 2.5M NaCl, 1% Triton X-100, 10% dimethyl sulfoxide, and 10 mM Tris, pH 10) for 1 h at 4℃. The slides were equilibrated with electrophoresis buffer (1 mM Na_2EDTA and 300 mM NaOH, pH 13) for 20 min preceding electrophoresis (25V, 35 min at room temperature). Subsequently, the slides were rinsed 3 times with neutralizing buffer (0.4 M Tris, pH 7.4) at 5-minute intervals. Upon the replacement of coverslips, slides were viewed using an Olympus IX51 inverted microscope (Shinjuku City, Tokyo, Japan) with excitation 510-560 nm, emission 590 nm. Images of 50 cells and comets were captured using Life Science-Olympus Soft Imaging Solutions v5 (Shinjuku City, Tokyo, Japan). Comet lengths were measured and reported in µm as average tail lengths.

Hoechst assay

HEK293 cells were cultured and grown to confluency (70%), and treated (control, IC_{25}, and IC_{50}) for 24 h [20, 21]. The cells were washed thrice in 0.1 M PBS and preserved with 10% paraformaldehyde (pH 7.4) for 5 min at 37℃. The removal of the fixative was facilitated by three 5 mL washes with 0.1 M PBS. After removal of PBS, 1,000 µL of Hoechst 33342 working solution (5 µL of Hoechst dye in 10 mL PBS) (Sigma-Aldrich, St. Louis, Missouri, USA) was added in each flask. The flasks were incubated at 37℃ for 15 min, then washed with PBS and viewed under an Olympus IX51 inverted microscope with 350 nm excitation and 450 nm emission filters. Five images per control and treatment were captured at 200× magnification utilizing the Life Science-Olympus Soft Imaging Solutions v5.

Thiobarbituric acid reactive substances (TBARS) assay

Malondialdehyde, the end-product of lipid peroxidation by ROS, was quantified using the TBARS assay [20, 21]. Glass test tubes were appropriately labeled (control, IC_{25}, and IC_{50}) for this assay. Then each tube received 200 µL of supernatant from previously treated samples. The positive (199 µL CCM + 1 µL malondialdehyde

(MDA) (Merck, Darmstadt, Germany)) and negative controls (200 µL CCM) were prepared in 2 other glass tubes. Subsequently, 200 µL of 2% and 7% of phosphoric acid was added to each test tube followed by 400 µL of TBA/butylated hydroxytoluene solution to every sample except the blank (negative control). The glass tubes were transiently vortexed, and pH was adjusted using 1 M HCl (200 µL). Boiling the samples in a water bath for 15 min at 100°C facilitated the optimal hydrolysis of MDA adducts. Butanol (1,500 µL) was then added to cool the samples. Tubes were vortexed (30 s) and allowed to stand until the two distinct phases became apparent. To a 96-well plate, 200 µL of the butanol phase of each sample was pipetted in duplicate and was successively read *via* the Bio-Tek Quant MQ×200 spectrophotometer at 532 nm/600 nm. The average of 2 replicates was calculated and divided by the absorption coefficient (156/mM) to determine the average concentration of MDA (µM).

Nitrates assay

Production of reactive nitrogen species (RNS) was assessed using the nitrates assay [20, 21]. A concentration range of 0-200 µM (0, 3.125, 6.25, 12.5, 25, 50, 100, 200 µM) sodium nitrite standards was prepared. To a 96-well microtiter plate, 50 µL of each standard and sample supernatant was pipetted in duplicate. 50 µL of vanadium (III) chloride, 25 µL of sulfanilamide, and 50 µL of N-1-naphthyl ethylenediamine dihydrochloride (Merck, Darmstadt, Germany) were then added and incubated at 37°C for 45 min. The plate was read *via* the Bio-Tek µQuant MQ×200 spectrophotometer at 540 nm/690 nm. A standard curve was prepared, and the nitrate concentration was extrapolated from the equation generated.

Western blotting

Western blotting was used to assess the protein expression of the antioxidant and cell death response to allicin [20–22]. Crude protein was isolated from HEK293 cells (treated with IC_{25} and IC_{50} concentrations of allicin) using Cytobuster™ (Sigma-Aldrich, St. Louis, Missouri, USA) enriched with Roche protease (05892791001) and phosphatase inhibitors (04906837001) (Roche Diagnostics, Basel, Switzerland). The crude protein was quantified using the bicinchoninic acid (BCA) (Sigma-Aldrich, St. Louis, Missouri, USA) method. Standardized proteins (1 mg/mL) were denatured in Laemmli buffer (5×: 0.5 M Tris-HCl, pH 6.8, glycerol, 10% SDS, β-mercaptoethanol, 1% bromophenol blue), separated on SDS polyacrylamide gels (10% resolving gel and 4% stacking gel) for 90 min at 150 V and transferred onto nitrocellulose membranes using the Transblot® Turbo™ Transfer system (Bio-Rad, Hercules, California, USA). Membranes were then blocked with 5% BSA/milk in Tris-buffered saline (TTBS, 25 mM Tris, 150 mM NaCl, 0.05% Tween 20, pH 7.5) for 2 h, and incubated with primary antibody (cleaved PARP-1 (9542), p53 (48818), Bax (5023), SOD2 (13141), Nrf2 (12721); 1:1,000 in 5% BSA/TTBS (Cell Signaling Technology, Danvers, Massachusetts, USA)) overnight. After incubation, the primary antibody was removed; membranes were washed five times with TTBS (10 min each) and incubated with horseradish peroxidase (HRP) labeled secondary antibodies (anti-rabbit IgG or anti-mouse IgG in 5% BSA (1:2,000) (Cell Signaling Technology, Danvers, Massachusetts, USA)) for 2 h. Following incubation, membranes were washed with TTBS. Clarity Western ECL Substrate (Bio-Rad, Hercules, California, USA) (150 µL) was added to the membranes and images were captured using the Molecular Imager® Chemidoc™ XRS+ Bio-Rad imaging system (Hercules, California, USA). Band intensity was also determined using Image Lab™ Software v6.0 (Bio-Rad, Hercules, California, USA). Membranes were rinsed with 10 mL of dH_2O, quenched with 5 mL of hydrogen peroxide (H_2O_2) at 37°C for 30 min and re-probed with the house-keeping protein (HRP-conjugated anti-β-actin) (Sigma-Aldrich, St. Louis, Missouri, USA). Images were captured and analyzed by dividing the band intensity of each sample by the respective loading controls to determine relative band density.

Statistical analysis

All results were expressed as mean ± SD of two independent experiments. Statistical analysis was executed utilizing GraphPad Prism v.5.0 (GraphPad Software Inc., La Jolla, California, USA). The one-way analysis of variance test (ANOVA) with Bonferroni post-test or the unpaired t-test with Welch's correction was performed to determine statistical significance. The significance of the data was reported at P<0.05.

Results

Effect of allicin on cell viability

Cell viability decreased with increasing allicin concentration (2.5-150 µM); only 1 µM allicin resulted in increased cell viability (114%, Figure 1) relative to the control (100%). After yielding 96% viability at 2.5 µM allicin, the viability remained low (13%-28%) for 5-150 µM allicin treatments. IC_{50} (3.91 µM) and IC_{25} (1.96 µM) values were obtained and used in all subsequent assays (Figure 1).

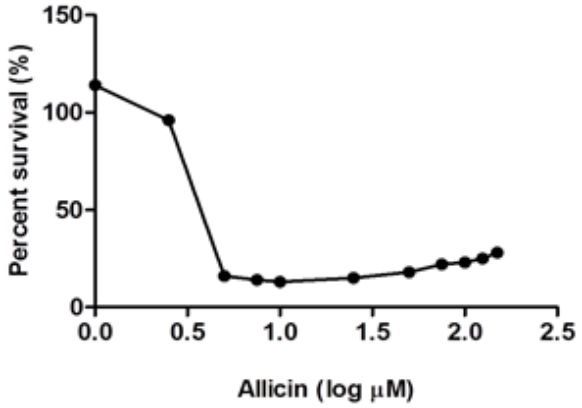

Figure 1. Cell viability of HEK293 cells after treatment of allicin. The data are expressed as mean ± SD of three independent experiments.

Induction of oxidative stress by allicin

Untreated cells yielded a nitrate concentration of 1.33 ± 0.02 µM. A 9.09-fold increase in nitrate concentration was observed for allicin at the IC_{25} concentration, which was further significantly increased (14-fold) at the IC_{50} concentration (P < 0.05) (Figure 2). Lipid peroxidation occurred following treatment with allicin. A non-significant increase in MDA concentration from 0.04 ± 0.01 µM in the control to 0.07 ± 0.01 µM at the IC_{25} concentration was noted, while a significant increase 0.17 ± 0.03 µM occurred at the IC_{50} concentration of allicin (P < 0.01) (Figure 3).

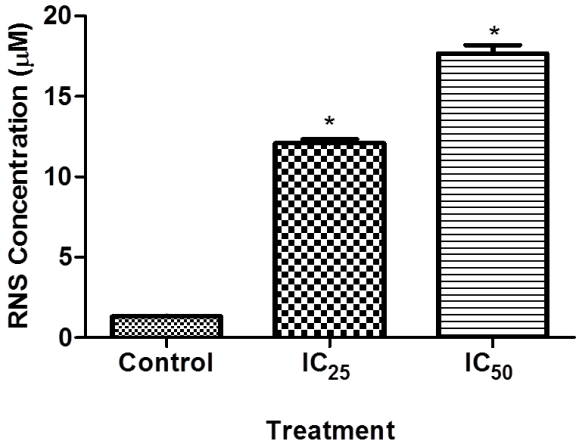

Figure 2. Allicin treated HEK293 cells with an IC_{25}-1.95 µM and IC_{50}-3.91 µM showed an overall escalation of reactive nitrogen species compared to the untreated HEK293 cells, which is indicative of nitrosative stress. *P < 0.05.

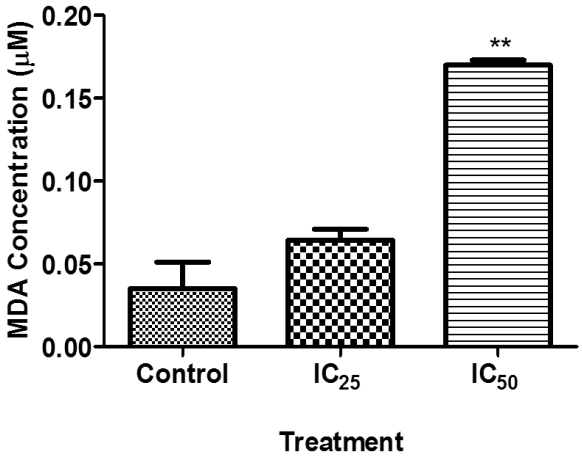

Figure 3. Malondialdehyde concentration of allicin treated HEK293 cells was seen to markedly increase. Lipid peroxidation was particularly increased at the IC_{50} treatment in comparison to the control. **P < 0.01.

Effect of allicin on caspase activity

At the IC_{25} concentration, a 3.09-fold increase was observed for initiator caspase 8, while a 1.97-

fold increase was shown in cells treated with IC_{50} concentration of allicin (Figure 4A), in comparison to the control. The same trend was noted for initiator caspase 9 at the IC_{25} and IC_{50} treated cells (Figure 4B). Executioner caspase 3/7 displayed a non-significant increase in caspase activity for both treatments (Figure 4C).

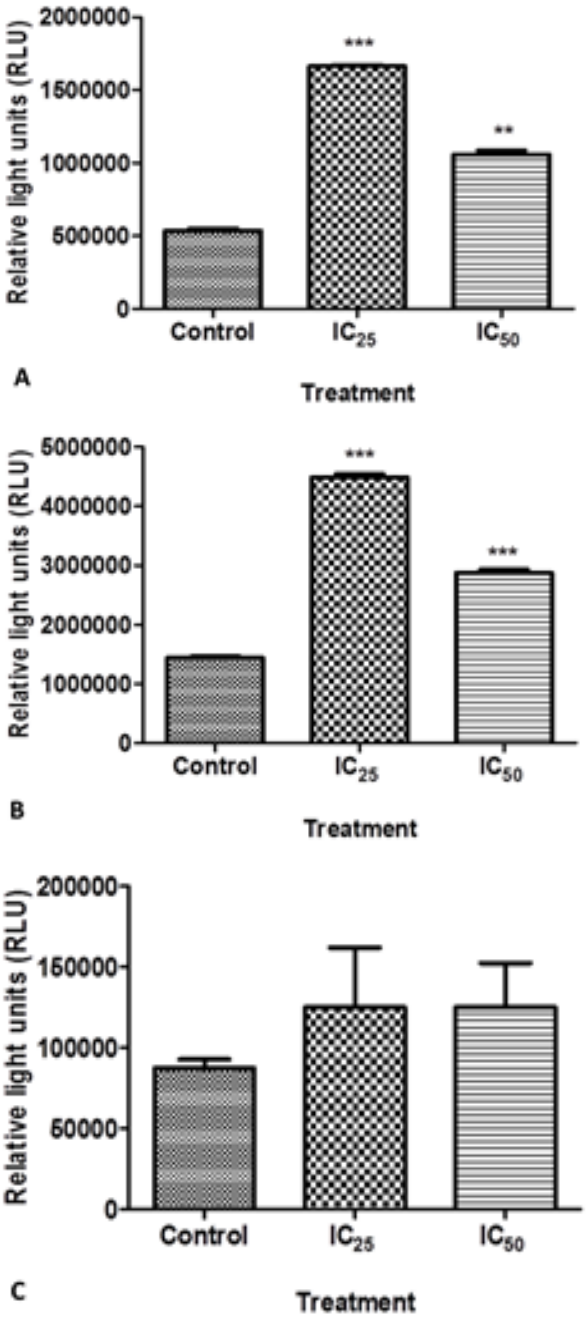

Figure 4. Effect of allicin on caspase activity in HEK293 cells. **A.** Caspase 8, **B.** Caspase 9, **C.** Caspases 3/7. ***P* < 0.01, ****P* < 0.001.

Effect of allicin on ATP level

Allicin induced elevated ATP levels at both concentrations compared to the control. A significant 2.75-fold increase was noted at the IC_{25} concentration (*P* < 0.001) while a 1.75-fold increase at the IC_{50} concentration (*P* < 0.001) (Figure 5).

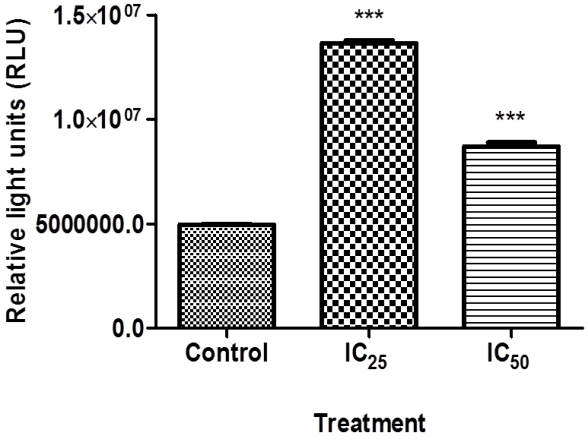

Figure 5. ATP levels were observed to be significantly elevated in allicin treated HEK293 cells relative to the control, with a marked increase in IC_{25} treated cells. ****P* < 0.001.

DNA damage

Tail length increased dose-dependently in cells treated with allicin (Figure 6). This was verified by the migration of DNA forming comet tails in treated cells (Figure 6B), relative to the intact core of DNA in the control group.

Late stages of apoptosis

DNA fragmentation and formation of apoptotic bodies are particularly characterized by late phases of apoptosis. Normal morphology of cells was observed in the control group (Figure 7A). However, allicin treatment resulted in apoptotic cells as shown in Figure 7B and 7C.

Antioxidant response and apoptotic induction

Allicin induced a 1.27-fold decline of the antioxidant regulator (Nrf2) at the IC_{25} concentration, while the expression of Nrf2 was increased by 1.14-fold at the IC_{50} concentration relative to the control (Figure 8A). SOD2 was upregulated dose-dependently by 1.22-fold and

A

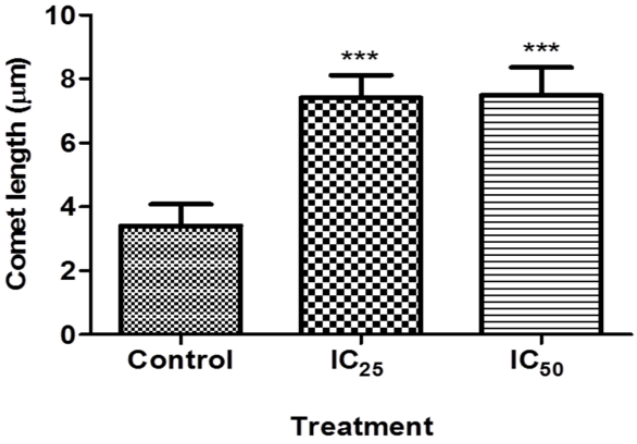

B

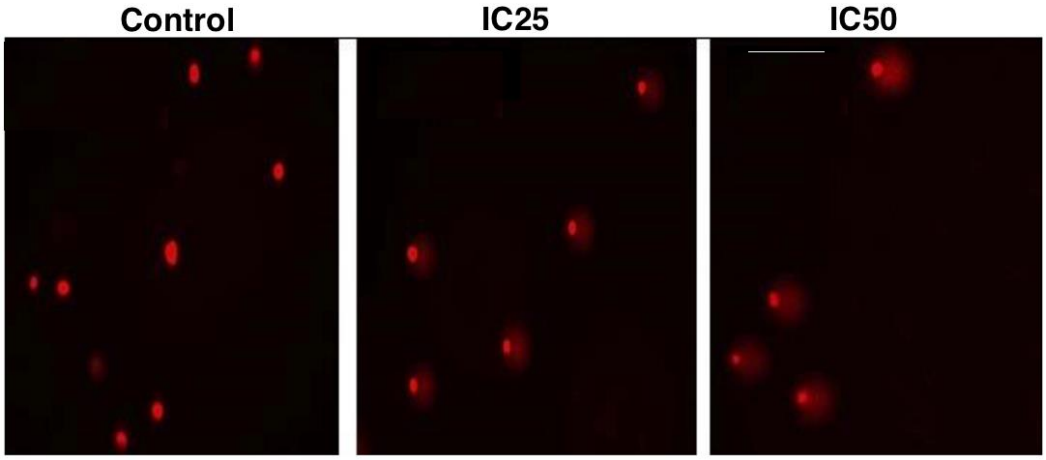

Figure 6. Effect of allicin on DNA damage by comet assay. **A.** A bar graph for comet length. Allicin-treated HEK293 cells display a similar increase in comet tail length comparing to the control. **B.** DNA damage in HEK293 cells treated with allicin. Comet tail length is directly correlated to DNA fragmentation and hence DNA damage. This was shown by the longer comet tail lengths in IC_{25} and IC_{50} treated cells relative to the intact DNA in the untreated HEK293 cells (200×). All the IC_{25} and IC_{50} treated cells had comet tails. ***$P < 0.001$ comparing to the control.

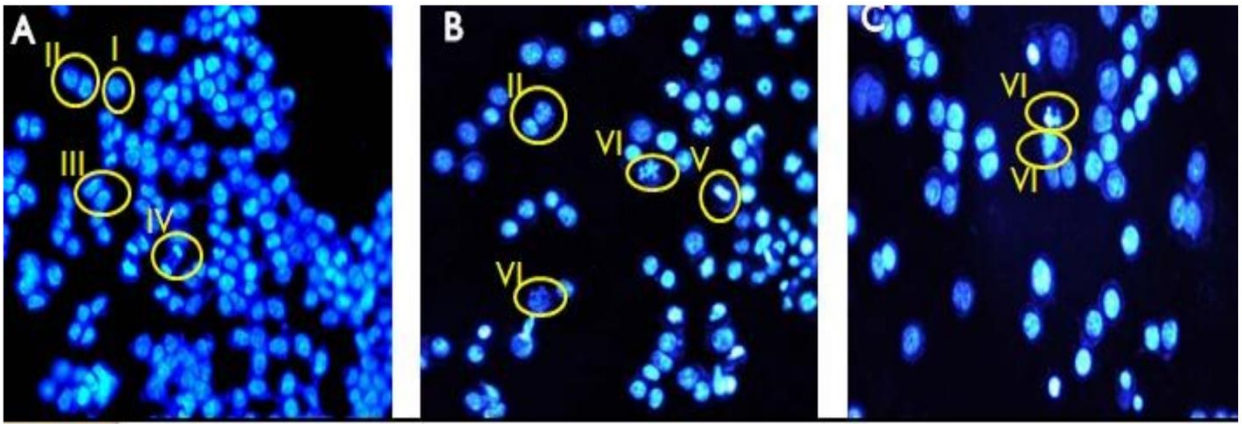

Figure 7. Nuclear morphology of allicin treated HEK293 cells. **A.** Untreated HEK293 cells. **B.** HEK293 cells treated with allicin at the IC_{25} concentration. **C.** HEK293 cells treated with allicin at the IC_{50} concentration. (I) prophase, (II) cytokinesis, (III) anaphase, (IV) telophase, (V) metaphase, (VI) apoptotic cells.

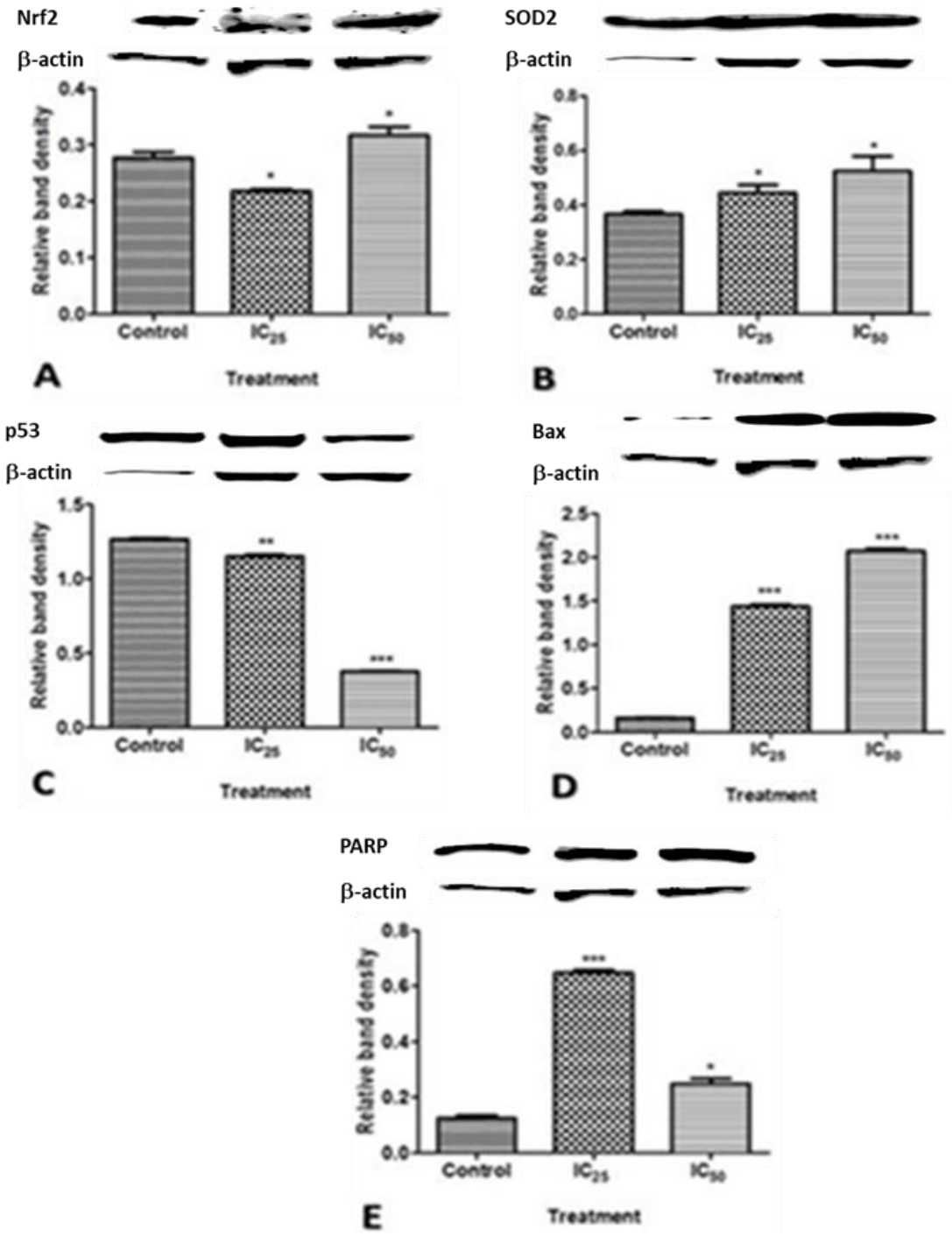

Figure 8. Protein expression of Nrf2 (**A**), SOD2 (**B**), p53(**C**), Bax (**D**), and PARP-1 (**E**) in allicin treated HEK293 cells. **P* < 0.05, ***P* < 0.01, ****P* < 0.001 comparing to the control.

1.43-fold after allicin treatments (IC_{25} and IC_{50}), respectively in comparison to untreated cells (Figure 8B). Expression of Bax was upregulated remarkably by allicin treatment (Figure 8D); however, its regulator p53 was down-regulated, especially at the IC_{50} concentration (Figure 8C). PARP-1 was shown to be cleaved and its level was increased in allicin treated cells. Allicin at the IC_{25}

concentration upregulated the expression of PARP-1 more significantly than that at the IC_{50} concentration (Figure 8E).

Discussion

This study was conducted to investigate the cytotoxic effect of allicin in HEK293 cells by using the IC_{50} in HEK293 cells, given its role as a possible therapeutic for a range of diseases including high blood pressure and cancer. Results revealed a rapid decline of viability and proliferation of cells dose-dependently (0-150 µM), obtaining an IC_{50} of 3.91 µM, from which the IC_{25} of 1.95 µM was derived. The decreased cell viability indicated by diminished formazan conversion was the first sign of toxicity induced in allicin-treated HEK293 cells as the obtained IC_{25} and IC_{50} were 94-fold and 47-fold lower than that of the organism dose (184 µM) that equivalents to the dose that a human takes each day.

A decline in cell viability can be attributed to the damage of cells, as a result of the collaboration between increased RNS and ROS activities. Free radicals generated such as superoxide anion ($O_2^{\bullet-}$) can be converted to H_2O_2 spontaneously or enzymatically *via* the enzyme SOD. The H_2O_2 generated is subsequently converted to H_2O by glutathione peroxidase (GPx)/catalase. However, if there is a lack of GPx/catalase activity, the H_2O_2 produced can be transformed to the highly reactive hydroxyl radical ($OH^{\bullet}$) *via* the Fenton reaction in the presence of metal ions [12, 23]. In this study, the upregulation of SOD2 was displayed in a dose-dependent manner. This would result in increased H_2O_2 requiring detoxification. However, the entry of high concentrations of allicin into the cell reacts with and oxidizes GSH and cysteine residues hence reducing the GSH pool. Reduced GSH could further lead to the incapacitation of GPx in detoxifying elevated quantities of H_2O_2 produced by SOD2, exacerbating the progression of free radicals.

As a consequence of unrestrained oxidative stress *i.e.* when the antioxidant capacity becomes overwhelmed by increased ROS/RNS production, injury to organs, tissues, and cells are displayed. In particular, direct destruction to lipids has been correlated to elevated ROS/RNS [23]. Reactive nitrogen species (RNS) forms when $O2^{\bullet-}$ and nitrogen oxide (NOX) react, giving rise to the reactive peroxynitrite (ONOO) and successive lipid peroxidation [24, 25]. In results obtained, allicin drastically increased nitrate and nitrite concentrations in HEK293 cells with increasing dose, measured by the nitrates assay, which is an indirect indicator of RNS in the cell. Allicin treatments also significantly raised MDA concentration, which is the end-product of lipid peroxidation measured using the TBARS assay. This suggests that allicin-induced ROS/RNS production may be associated with subsequent lipid damage, therefore, proving the oxidant nature of allicin in HEK293 cells. In studies conducted by Luo *et al*. and Gruhlke *et al*., it was shown that allicin resulted in the generation of ROS as well as DNA damage in a short time [8, 17].

While allicin can be described chemically as an oxidant because of its oxidizing properties, particularly thiolate ions, the Allium genus can be deemed for its antioxidant effects in explicit concentrations. Allicin however does display its antioxidant role physiologically, as mentioned by the instigation of phase two detoxification system and antioxidant proteins *via* the activation of Nrf2 [8]. Nrf2 is primarily responsible for regulating the initiation of these genes. In oxidative stress conditions or cellular stimulation by electrophiles such as allicin [26], Nrf2 gets dissociated from kelch-like ECH associating protein 1 (Keap-1) and translocates to the nucleus where it triggers the transcription of genes related to the antioxidant response, including SOD and GSH [16, 27]. In this study, results showed a decrease in Nrf2 expression at the IC_{25} concentration of allicin, but a sharp increase at the IC_{50} concentration, which indicated that increased expression of Nrf2 was required for a higher concentration to combat

the oxidant response. This was substantiated through studies conducted by Bat-Chen *et al*. who showed that Nrf2 protein plays a crucial role in the cytotoxicity induced by allicin in colon cancer cells at a concentration of 10 µg/mL [16].

Although Nrf2 is shown as a mediator of antioxidant response in elevated stress conditions, this was not enough to overcome allicin induced oxidant levels, which resulted in cell death. Evidence shows that allicin-mediated cytotoxicity through increased ROS production decreases the outer mitochondrial membrane potential and as a consequence result in the leakage of apoptogenic molecules such as Cytochrome C from the mitochondria [16, 17, 28]. Previous studies have also revealed that the impediment of cancer cell development by allicin directly coincides with apoptosis induction *via* the activation of initiator caspase-8, -9, and executioner caspase 3[29].

Apoptosis is commonly referred to as programmed cell death and is mediated predominantly by caspase-activation in two pathways, extrinsic or intrinsic mitochondrial pathway [30]. The extrinsic pathway is stimulated when FAS ligand binds to its receptor and results in the activation of caspase 8; this proceeds to activate other caspases [31]. Also, it can activate t-bid, a BH3 only protein, which goes on to trigger the mitochondrial pathway, which is governed by pro-apoptotic and anti-apoptotic factors. When pro-apoptotic proteins such as Bax are activated, it can facilitate the release of Cytochrome C which binds to apoptotic protease activating factor 1 protein and pro-caspase 9, resulting in caspase 9 auto-activation [17, 32]. The initiator caspases of both the extrinsic and intrinsic pathways activate the executioner caspase 3/7 that is crucial for the fragmentation of DNA. Both caspases 8 and 9 were markedly elevated in comparison to the control whereas caspase 3/7 showed a transient increase in allicin treated cells.

Coherently, results in the study exhibited a significant upregulation of Bax in HEK293 cells dose-dependently, indicating that allicin mediated apoptosis by the release of Cytochrome C *via* the mitochondrial pathway. The expression of p53, a regulator of Bax, was decreased by allicin. It seems that allicin stimulates pro-apoptotic proteins without p53 in HEK293 cells. This can be supported by an experiment conducted by Bat-Chen *et al*., in which allicin affected the ratio of anti-apoptotic (Bcl-2 which was down-regulated) to pro-apoptotic (Bax shown to be upregulated) proteins of the Bcl-2 family in human colon cancer cells (HCT116) [16]. The effect in this experiment was correlated with the loss of the mitochondrial membrane potential, resulting in the release of molecules such as Cytochrome C.

Mitochondria function in the production of energy to sustain cells and facilitate cell death processes [33]. Effector caspase stimulation, signaling of kinases, and apoptosome formation are energy-reliant steps crucial for the implementation of the apoptotic program. The increase in ATP as observed in the study confirmed the availability of energy to facilitate allicin-induced apoptotic cell death. The mechanism of ATP-induced apoptotic cell death is through several highly regulated processes that are ATP-dependent such as caspase activation, enzymatic hydrolysis of macromolecules, bleb formation, and apoptotic body formation. The elevated caspase 8 and 9 activities coupled with the increased ATP activity and apoptotic cell death in allicin treated HEK293 cells support the hypothesis that an increase in ATP induces apoptotic cell death whiles depletion of ATP may cause the switching of the cell death from apoptosis to necrosis. Therefore, the levels of ATP determine the type of cell death [33, 34].

A hallmark of apoptosis is the fragmentation of DNA which is caused through both caspase-dependent and caspase-independent mechanisms [34]. Cleaved caspase 3 translocation to the nucleus and subsequent cleavage of the enzyme PARP is caspase reliant [35]. PARP-1 is most commonly involved in the repair of DNA damage as well as the modification

of nuclear proteins [36]. Cleaved PARP-1 was increased following allicin treatment. This suggests that caspases played a role in the fragmentation of DNA through cleaved PARP-1 upregulation in the 89 kDa fragment.

The extent of DNA fragmentation in allicin treated HEK293 cells was shown by the comet tail length [37]. Cells treated with both IC_{25} and IC_{50} of allicin showed a distinct rise in tail length in contrast to the control cells and DNA fragmentation was induced in HEK293 cells. The master regulator p53 is renowned for many functions, among those is the initiation of DNA repair enzymes [38, 39]. The declined expression of p53 would, therefore, account for the fragmentation of DNA. The Hoechst assay confirmed these results, displaying a decrease in cell number relative to the control. Apoptotic cells were also evident in IC_{25} and IC_{50} treated cells in comparison to the control, which just presented normal cell cycle events. In view of the biological activities of allicin in HEK293 cells, it must, however, be noted that since this study was conducted using cell lines, the findings cannot be generalized to animal models as well as clinical experimentations involving humans and should, therefore, be verified in appropriate *in vivo* models in future studies. Furthermore, the study conducted involved the activity of different concentrations of allicin at the same time and, therefore, the findings of the study cannot be generalized for similar concentrations observed over different time intervals (24, 48, 72 h) as prolonged duration of activity may affect the therapeutic goals of allicin.

Conclusion

Allicin causes oxidative stress by increasing ROS and RNS. Its antioxidant nature was seen *via* upregulation of Nrf2 and transcription of SOD2. However, this effect was overwhelmed by its oxidant capacity at the IC_{50} value. As a result, cell death occurred *via* the apoptotic route through the activation of initiator and executioner caspases. Furthermore, allicin was found to stimulate pro-apoptotic proteins independent of p53 in HEK293 cells, established by the downregulation of p53 and upregulation of Bax. Cleavage of PARP-1 and a declined expression of p53 accounted for the DNA fragmentation in HEK293 cells, indicating that allicin is cytotoxic to HEK293 cells at higher concentrations. Hence, future studies should include the same concentration of allicin at different time intervals (24, 48, 72 h) to observe variations in its response, as time and concentration have been noted to be two key factors implicated in allicin-mediated effects. Additionally, future studies must be conducted in appropriate animal models for the verification of the activities of allicin *in vivo* and its subsequent activities in clinical experimentations involving humans where applicable.

Acknowledgments

The financial assistance of the National Research Foundation towards this research is hereby acknowledged. Opinions expressed and conclusions arrived at, are of those of the author and are not necessarily to be attributed to the National Research Foundation.

References

1. Borlinghaus J, Albrecht F, Gruhlke M, Nwachukwu I, Slusarenko A. 2014. Allicin: Chemistry and Biological Properties. Molecules. 19:12591–12618.
2. Yuan H, Ma Q, Ye L, Piao G. 2016. The Traditional Medicine and Modern Medicine from Natural Products. Molecules. 21:559.
3. Omar SH, Al-Wabel NA. 2010. Organosulfur compounds and possible mechanism of garlic in cancer. Saudi Pharm J. 18:51–58.
4. Sener G, Sakarcan A, Yeğen BÇ. 2007. Role of garlic in the prevention of ischemia-reperfusion injury. Mol Nutr Food Res. 51:1345–1352.
5. Vazquez-Prieto MA, Miatello RM. 2010. Organosulfur compounds and cardiovascular disease. Mol Aspects Med. 31:540–545.
6. Goncharov N, Orekhov AN, Voitenko N, Ukolov A, Jenkins R, Avdonin P. Organosulfur Compounds as Nutraceuticals. In: Nutraceuticals. Elsevier; 2016:555–568.
7. Block E. 2005. Biological activity of allium compounds: Recent results. Acta Hortic. 688:41–58.

8. Gruhlke M, Nicco C, Batteux F, Slusarenko A. 2016. The Effects of Allicin, a Reactive Sulfur Species from Garlic, on a Selection of Mammalian Cell Lines. Antioxidants. 6:1–17.
9. Wall SB, Oh J-Y, Diers AR, Landar A. 2012. Oxidative Modification of Proteins: An Emerging Mechanism of Cell Signaling. Front Physiol. 3:369.
10. Fra A, Yoboue ED, Sitia R. 2017. Cysteines as Redox Molecular Switches and Targets of Disease. Front Mol Neurosci. 10:167.
11. Mikaili P, Maadirad S, Moloudizargari M, Aghajanshakeri S, Sarahroodi S. 2013. Therapeutic uses and pharmacological properties of garlic, shallot, and their biologically active compounds. Iran J Basic Med Sci. 16(10):1031-1048.
12. Nicco C, Batteux F. 2017. ROS Modulator Molecules with Therapeutic Potential in Cancers Treatments. Molecules. 23:84.
13. Amagase H. 2006. Clarifying the Real Bioactive Constituents of Garlic. J Nutr. 136:716S-725S.
14. Bayan L, Koulivand PH, Gorji A. 2014. Garlic: a review of potential therapeutic effects. Avicenna J phytomedicine. 4:1–14.
15. Bhandari P. 2012. Garlic (*Allium sativum* L.): A review of potential therapeutic applications. Int J Green Pharm. 6:118.
16. Bat-Chen W, Golan T, Peri I, Ludmer Z, Schwartz B. 2010. Allicin Purified from Fresh Garlic Cloves Induces Apoptosis in Colon Cancer Cells *via* Nrf2. Nutr Cancer. 62:947–957.
17. Luo R, Fang D, Hang H, Tang Z. 2016. The Mechanism in Gastric Cancer Chemoprevention by Allicin. Anticancer Agents Med Chem. 16:802–809.
18. Orrenius S, Nicotera P, Zhivotovsky B. 2011. Cell Death Mechanisms and Their Implications in Toxicology. Toxicol Sci. 119:3–19.
19. Morales J, Li L, Fattah FJ, Dong Y, Bey EA, Patel M, *et al*. 2014. Review of Poly (ADP-ribose) Polymerase (PARP) Mechanisms of Action and Rationale for Targeting in Cancer and Other Diseases. Crit Rev Eukaryot Gene Expr. 24:15–28.
20. Satyo L, Amoako DG, Somboro AM, Sosibo SC, Kumalo HM, Mhlongo NN, *et al*. 2020. Molecular Insights into Di(2-Picolyl) Amine–Induced Cytotoxicity and Apoptosis in Human Kidney (HEK293) Cells. Int J Toxicol. 39:341–351.
21. Perumal PO, Mhlanga P, Somboro AM, Amoako DG, Khumalo HM, Khan RM. 2019. Cytoproliferative and Anti-Oxidant Effects Induced by Tannic Acid in Human Embryonic Kidney (Hek-293) Cells. Biomolecules. 9:767.
22. Tsotetsi N, Amoako DG, Somboro AM, Khumalo HM, Khan RB. 2020. Molecular mechanisms underlying the renoprotective effects of 1,4,7-triazacyclononane: a βeta-lactamase inhibitor. Cytotechnology. 72:785–796.
23. Kurutas EB. 2015. The importance of antioxidants which play the role in cellular response against oxidative/nitrosative stress: current state. Nutr J. 15:71.
24. Phaniendra A, Jestadi DB, Periyasamy L. 2015. Free Radicals: Properties, Sources, Targets, and Their Implication in Various Diseases. Indian J Clin Biochem. 30:11–26.
25. Ozcan A, Ogun M. Biochemistry of Reactive Oxygen and Nitrogen Species. In: Basic Principles and Clinical Significance of Oxidative Stress. InTech; 2015:23–67.
26. Vomund S, Schäfer A, Parnham M, Brüne B, von Knethen A. 2017. Nrf2, the Master Regulator of Anti-Oxidative Responses. Int J Mol Sci. 18:2772.
27. Lu M-C, Ji J-A, Jiang Z-Y, You Q-D. 2016. The Keap1-Nrf2-ARE Pathway As a Potential Preventive and Therapeutic Target: An Update. Med Res Rev. 36:924–963.
28. Cheng J, Nanayakkara G, Shao Y, Cueto R, Wang L, Yang WY, *et al*. 2017. Mitochondrial Proton Leak Plays a Critical Role in Pathogenesis of Cardiovascular Diseases. Adv Exp Med Biol. 982:359-370.
29. Zhang W, Ha M, Gong Y, Xu Y, Dong N, Yuan Y. 2010. Allicin induces apoptosis in gastric cancer cells through activation of both extrinsic and intrinsic pathways. Oncol Rep. 24:1585–1592.
30. Hassan M, Watari H, AbuAlmaaty A, Ohba Y, Sakuragi N. 2014. Apoptosis and Molecular Targeting Therapy in Cancer. Biomed Res Int. 2014:1–23.
31. Parrish AB, Freel CD, Kornbluth S. 2013. Cellular Mechanisms Controlling Caspase Activation and Function. Cold Spring Harb Perspect Biol. 5:a008672–a008672.
32. Riedl SJ, Shi Y. 2004. Molecular mechanisms of caspase regulation during apoptosis. Nat Rev Mol Cell Biol. 5:897–907.
33. Kushnareva Y, Newmeyer DD. 2010. Bioenergetics and cell death. Ann N Y Acad Sci. 1201:50–57.
34. McIlwain DR, Berger T, Mak TW. 2013. Caspase Functions in Cell Death and Disease. Cold Spring Harb Perspect Biol. 5:a008656–a008656.
35. Kitazumi I, Tsukahara M. 2011. Regulation of DNA fragmentation: the role of caspases and phosphorylation. FEBS J. 278:427–441.
36. Lyakhovich A, Surralles J. 2010. Constitutive Activation of Caspase-3 and Poly ADP Ribose Polymerase Cleavage in Fanconi Anemia Cells. Mol Cancer Res. 8:46–56.
37. Kumaravel TS, Vilhar B, Faux SP, Jha AN. 2009. Comet Assay measurements: a perspective. Cell Biol Toxicol. 25:53–64.
38. Hafner A, Bulyk ML, Jambhekar A, Lahav G. 2019. The multiple mechanisms that regulate p53 activity and cell fate. Nat Rev Mol Cell Biol. 20:199–210.
39. Farnebo M, Bykov VJN, Wiman KG. 2010. The p53 tumor suppressor: A master regulator of diverse cellular processes and therapeutic target in cancer. Biochem Biophys Res Commun. 396:85–89.